HHS Public Access

Author manuscript

Exp Eye Res. Author manuscript; available in PMC 2022 July 03.

Published in final edited form as:

Exp Eye Res. 2021 June ; 207: 108610. doi:10.1016/j.exer.2021.108610.

The functional role of decorin in corneal neovascularization *in vivo*☆

Praveen K. Balne[a,b], **Suneel Gupta**[a,b], **Jinjin Zhang**[a,b], **Daniel Bristow**[a,b,c], **Matthew Faubion**[a,b,c], **Sally D. Heil**[a,b], **Prashant R. Sinha**[a,b], **Sydney L. Green**[a,b], **Renato V. Iozzo**[d], **Rajiv R. Mohan**[a,b,c,*]

[a]Harry S. Truman Memorial Veterans' Hospital, Columbia, MO, United States

[b]One-Health Vision Research Program, Departments of Veterinary Medicine & Surgery and Biomedical Sciences, College of Veterinary Medicine, University of Missouri, Columbia, MO, United States

[c]Mason Eye Institute, School of Medicine, University of Missouri, Columbia, MO, United States

[d]Department of Pathology, Anatomy, and Cell Biology, and the Translational Cellular Oncology Program, Sidney Kimmel Medical College at Thomas Jefferson University, Philadelphia, Pennsylvania, United States

Abstract

Our earlier *decorin* (*Dcn*) gene overexpression studies found that the targeted *Dcn* gene transfer into the cornea inhibited corneal angiogenesis *in vivo* using a rabbit model. In this study, we tested the hypothesis that anti- angiogenic effects of decorin in the cornea are mediated by alterations in a normal physiologic balance of pro- and anti-angiogenic factors using decorin deficient (*Dcn* $^{-/-}$) and wild type (*Dcn* $^{+/+}$) mice. Corneal neovascularization (CNV) in *Dcn* $^{-/-}$ and *Dcn* $^{+/+}$ mice was produced with a standard chemical injury technique. The clinical progression of CNV in mice was monitored with stereo- and slit-lamp microscopes, and histopathological hematoxylin and eosin (H&E) staining. Protein and mRNA expression of pro- and anti-angiogenic factors in the cornea were evaluated using immunofluorescence and quantitative real-time PCR, respectively. Slit-lamp clinical eye examinations revealed significantly more CNV in *Dcn*$^{-/-}$ mice than the *Dcn* $^{+/+}$ mice post-injury ($p < 0.05$) and AAV5-*Dcn* gene therapy significantly reduced CNV in *Dcn*$^{-/-}$ mice compered to no AAV5-*Dcn* gene therapy controls ($p < 0.001$). H&E-stained corneal sections exhibited morphology with several neovessels in injured corneas of the *Dcn* $^{-/-}$ mice than the *Dcn* $^{+/+}$ mice. Immunofluorescence of corneal sections displayed significantly higher expression of α-smooth muscle actin (*α-SMA*) and endoglin proteins in *Dcn*$^{-/-}$ mice than *Dcn* $^{+/+}$ mice ($p < 0.05$). Quantitative real-time PCR found significantly increased mRNA levels of pro-angiogenic factors *endoglin* (2.53-fold; $p < 0.05$), *Vegf* (2.47-fold; $p < 0.05$), and *Pecam* (2.14-fold; $p < 0.05$) and anti-angiogenic factor *Vegfr2* (1.56-fold; $p < 0.05$) in the normal cornea of the *Dcn* $^{-/-}$ mice than the *Dcn* $^{+/+}$ mice. Furthermore, neovascularized *Dcn* $^{-/-}$ mice corneas showed greater increase in mRNA expression of pro-angiogenic factors *endoglin* (4.58-fold; $p <$

☆Declarations of interest: None.

*Corresponding author. FARVO Professor of Ophthalmology and Molecular Medicine University of Missouri, 1600 E. Rollins St, Columbia, MO 65211, United States. mohanr@health.missouri.edu (R.R. Mohan). .

0.0001), *Vegf* (4.16-fold; $p < 0.0001$), *and Pdgf* (2.15-fold; $p < 0.0001$) and reduced expression of anti-angiogenic factors *Ang2* (0.12-fold; $p < 0.05$), *Timp1* (0.22-fold; $p < 0.05$), and *Vegfr2* (0.67-fold; $p > 0.05$) compared to neovascularized $Dcn^{+/+}$ mice corneas. These gene deficience studies carried with transgenic $Dcn^{-/-}$ mice revealed decorin's role in influencing a physiologic balance between pro-and anti- angiogenic factors in the normal and injured cornea. We infer that the functional deletion of *Dcn* promotes irregular corneal repair and aggravates CNV.

Keywords

Decorin; Cornea; Corneal neovascularization; Gene therapy; Pro-angiogenic factors; Anti-angiogenic factors

1. Introduction

Corneal neovascularization (CNV) affects the vision due to the formation of blood vessels and their invasion onto the corneal surface. CNV causes corneal surface irregularity, which leads to aberrations, edema, and finally, stromal opacification (Azar, 2006). A variety of etiologies including infection, injury, inflammation, ischemia, degeneration, limbal insufficiency, allergic eye diseases, chemical burns, and contact lens wearing can all cause CNV (Lee et al., 1998; Lim et al., 2009). CNV may be beneficial in certain pathological conditions such as clearing corneal infections, wound healing, and conditions involving stromal necrosis. However, CNV can cause corneal scarring, inflammation, edema, and affect the immune privilege of the cornea, leading to decreased visual acuity (Faraj et al., 2011). CNV is one of the primary risk factors for corneal graft failure (Bachmann et al., 2010).

Following corneal insult, the mechanism of CNV involves the secretion of proteases by endothelial cells, which degrade the basal membrane of the perilimbal capillary network. The extracellular matrix (ECM) is then invaded by migrated endothelial cells (ECs). ECs begin proliferation in the ECM. Finally, the lumina of the new blood vessels form, and the basal membrane is remodeled (Shi et al., 2010). CNV is a complex pathological process which involves several factors including vascular endothelial growth factor (VEGF), platelet-derived growth factor (PDGF), basic fibroblast growth factor (bFGF), hypoxia-inducible factor (HIF), Nitric oxide (NO), and matrix metalloproteinases (MMPs) through multiple pathways such as the RHO/ROCK pathway, Wnt pathway, and NOD1 pathway (Liu et al., 2017; Roshandel et al., 2018; Kim et al., 2013; Yin et al., 2007; Wang et al., 2015).

CNV management is primarily focused on the underlying etiology and pathophysiology of a given disease (Aydin et al., 2008). Cortico-steroids form the first-line therapeutics for treating CNV. However, prolonged use of corticosteroids can cause adverse side effects including cataracts, glaucoma, and infection (Aydin et al., 2008). Though anti-VEGF agents like bevacizumab have shown some promising results in treating CNV (Papathanassiou et al., 2013), they can cause side effects like delayed epithelial wound healing, upregulation of MMPs, persistent epithelial defects, and subconjunctival hemorrhage (Kim et al., 2009, 2013; Dekaris et al., 2015; and Petsoglou et al., 2013). Manipulation of genes involving in CNV pathogenesis is an alternative and promising approach for treating CNV.

Decorin (DCN) is a small leucine-rich proteoglycan (SLRP) that plays a key role in maintaining tissue homeostasis by regulating ECM synthesis, fibrillogenesis, and wound healing (Mohan et al., 2011a,b,c). DCN functions as an anti-fibrotic and anti-angiogenesis molecule by antagonizing transforming growth factor-beta (TGFβ) (Mohan et al., 2011a,b,c) and vascular endothelial growth factor A (Neill et al., 2012), respectively. In our earlier *Dcn* gene overexpression studies, adeno-associated virus (AAV) mediated tissue-targeted *Dcn* gene delivery into the corneal stroma significantly reduced CNV development without any negative side effects (Mohan et al., 2011a). *Dcn* gene therapy significantly ($p < 0.05$) down-regulated expression of pro-angiogenic factors VEGF, monocyte chemoattractant protein-1 (MCP1), and angiopoietin and up-regulated anti-angiogenic factor pigment epithelium-derived factor (PEDF) gene and significantly ($p < 0.05$) reduced CNV at early, mid, and late stages compared to no *Dcn* delivered control corneas (Mohan et al., 2011a). However, the functional role of DCN in regulating CNV is not fully understood. In this study, we tested our hypothesis that DCN's anti-angiogenic effects in the cornea are mediated by alterations in pro- and anti-angiogenic factors influencing a normal physiologic balance crucial of transparency maintenance using decorin deficient ($Dcn^{-/-}$) and wild type ($Dcn^{+/+}$) mice models.

2. Materials and methods

2.1. Animals

In this study, C57BL/6J decorin-deficient ($Dcn^{-/-}$) mice were generated from a breeding pair kindly provided by Professor Renato Iozzo, Sidney Kimmel Medical College, Thomas Jefferson University, Philadelphia, PA). Wild type C57BL/6J ($Dcn^{+/+}$) mice were purchased from the Jackson Laboratory, Bar Harbor, ME. Both, $Dcn^{+/+}$ and $Dcn^{-/-}$ mice were used to elucidate the functional role of decorin in corneal neovascularization *in vivo*. Male and female mice eight to twelve weeks in age, selected randomly, were used. The study was approved by the institutional ethics board and conducted following the declaration of tenets of Helsinki. Animal procedures were approved by the Animal Care and Use Committee of the University of Missouri, Columbia, and the Harry S. Truman Memorial Veterans' Hospital, Columbia, Missouri. All animals were treated, and experimental procedures were performed in adherence with the Association for Research in Vision and Ophthalmology (ARVO) statement for the use of animals in ophthalmic and vision research.

2.2. Induction of corneal neovascularization

Decorin-deficient ($Dcn^{-/-}$) mice (n = 10) (genetic background is C57BL/J6) and wild type C57BL/6J ($Dcn^{+/+}$) mice (n = 10) were bred by homozygote breeding. *Dcn* gene deficiency was confirmed by a polymerase chain reaction using specific primers for $Dcn^{-/-}$ mice PGK-1: 5'>TGG ATG TGG AAT GTG TGC GAG C <3' (position 2347–2368 in PGK promoter), Dec-5': 5'>CCT TCT GGC ACA AGT CTC TTG G <3' (position 245–266 in murine decorin cDNA), and Dec-3': 5'>TCG AAG ATG ACA CTG GCA TCG G <3' (Inv. Comp 384–405 in murine decorin cDNA). Corneal neovascularization was induced in both the $Dcn^{-/-}$ mice and $Dcn^{+/+}$ mice by a standard alkali burn injury method as described previously (Kitano et al., 2010). In brief, mice were anesthetized with an intraperitoneal injection of ketamine hydrochloride 100 mg/kg (JHP Pharmaceuticals, LLC, Rochester, MI,

USA) and xylazine hydrochloride 10 mg/kg (XylaMed, Bimeda Inc., IL, USA). For topical anesthesia, a single drop of proparacaine hydrochloride 0.5% solution (Alcon, Ft. Worth, TX, USA) was instilled into the eye. Corneal alkali injury was performed by placing a 2-mm diameter filter paper disc (P8, Filter Paper, Fisher Brand, Fisher Scientific, Pittsburgh, PA, USA), presoaked in Sodium hydroxide (NaOH) 0.5M solution (Sigma-Aldrich, St. Louis, MO, USA), onto the central cornea for 30 s, followed by extensive rinsing with balanced salt solution (Alcon, Fort Worth, TX) (Kitano et al., 2010). Alkali injury was performed in only one eye of each animal under the aid of a dissecting microscope (S6 E, Leica Microsystems Inc., Buffalo Grove, IL, USA), and the contralateral eye served as the naïve control (no alkali injury).

2.3. Corneal imaging

After alkali injury, all animals were imaged at day 0, 7, 14, and 21 post-injury for CNV progression assessment using a stereomicroscope (Leica DM 4000B, Leica Microsystems Inc., Buffalo Grove, IL, USA) equipped with a digital camera (SpotCam RT KE, Diagnostic Instruments Inc., Sterling Heights, MI, USA). The area of blood vessels in the cornea at day 21 post-injury in both the groups were quantified using NIH software Image J (Schneider et al., 2012). At day-21 post-injury, under ketamine/xylazine anesthesia, all animals were humanely euthanized with an intraperitoneal injection of pentobarbital 150 mg/kg (Diamondback Drugs, Scottsdale, AZ, USA).

2.4. Corneal tissue processing

Out of ten animals in each group, corneas from five animals were used for histology and immunofluorescence staining, and the remaining five animals were used for quantitative real-time polymerase chain reaction (qRT-PCR). Eyes were enucleated using sharp Westcott scissors and 0.12 forceps, embedded in optimal cutting temperature (OCT) compound (Sakura FineTek, Torrance, CA) within a 15 mm × 15 mm × 5 mm mold (Fisher, Pittsburgh, PA) and snap-frozen. The frozen tissue blocks were stored at − 80 °C until sectioning. Tissues were sectioned at 8 μm thickness using a Microm HM525 cryostat (Thermo Fisher Scientific, Waltham, MA) and mounted on microscopic glass slides (Superfrost Plus, Fisher Scientific, Pittsburgh, PA, USA) and stored at − 80 °C until hematoxylin and eosin staining and immunofluorescence staining were performed (Mohan et al., 2008). For qRT-PCR, corneas were dissected from the enucleated eyeballs, placed in 300 μL of RLT buffer (Qiagen, Valencia, CA), and stored at − 80 °C until RNA extraction.

2.5. Hematoxylin and eosin staining and immunofluorescence staining

Five alkali injured corneas and five naïve corneas from each group were used for both the hematoxylin and eosin (H&E) staining and Immunofluorescence staining. H&E staining was performed to assess the corneal structure before and after injury. This was done using the standard procedure for visualizing morphologic details, as previously reported (Tripathi et al., 2019). For immunofluorescence staining, tissue sections were rinsed in 1X PBS at room temperature for 5 min and outlined with a PAP pen. Tissue sections were incubated with 2% bovine serum albumin at room temperature for 30 min and subjected to immunostaining using primary antibodies for α-SMA (1:200 dilution, M0851; Dako, USA) at room temperature for 120 min, and endoglin (1:100 dilution, sc-18838, Santa Cruz, USA)

at 4 °C for overnight incubation separately. The tissue sections were then incubated with secondary antibodies Alexa Flour® 488 donkey anti-mouse IgG (1:500 dilution, A21202, Invitrogen, USA) and Alexa Flour® 594 goat anti-mouse IgG2a (1:500 dilution, A21135, Invitrogen, USA) for 45 min at room temperature in the dark for α-SMA and endoglin, respectively. Tissue sections were washed thrice in PBS+0.02% Tween 20, mounted in Vectashield containing 4′−6-diamidino-2-phenylindole (DAPI; Vector Laboratories, Inc. Burlingame, CA, USA), and photographed with Leica DM4000B fluorescent microscope (Leica Microsystems Inc., Illinois, USA) equipped with a digital camera (SpotCam RT KE, Diagnostic Instruments Inc., Sterling Heights, MI, USA). The immunostaining positive cells were quantified in six randomly selected, non-overlapping, full-thickness central corneal columns, extending from the anterior to the posterior stromal surfaces (Mohan et al., 2011a,c).

2.6. RNA extraction and cDNA synthesis

Total RNA was extracted from five alkali injured corneas and five naïve corneas from each group using a commercial RNA extraction kit (RNeasy Mini Kit from Qiagen, Valencia, CA) and cDNA was reverse transcribed using Avian Myeloblastosis Virus Reverse Transcriptase (AMV RT) (Promega, Madison, WI) following the manufacturer's guidelines (Tripathi et al., 2019).

2.7. Gene expression quantification by quantitative real-time polymerase chain reaction (qRT-PCR)

Pro-angiogenic factors *Vegf*, *Pdgf*, *Pecam* (platelet endothelial cell adhesion molecule), and *endoglin* and anti-angiogenic factors *Vegfr2* (VEGF receptor 2), *Timp1* (tissue inhibitor of metalloproteinases 1), and *Ang2* (Angiopoietin 2) mRNA expression were evaluated by quantitative real-time polymerase chain reaction (qRT-PCR) using the StepOnePlus™ Real-Time PCR System (Applied Biosystems, Carlsbad, CA). A qRT-PCR reaction mixture (20 μL) consisted of 200 nM of each forward primer (1 μL), reverse primer (1 μL), 10 μL 2X SYBR green supermix (Bio-Rad Laboratories, Hercules, CA), and 2 μL of cDNA. The primer sequences for qRT-PCR are listed in Table 1. The qPCR was performed at universal cycle conditions which include initial denaturation at 95 °C for 10 min, 40 cycles of denaturation at 95 °C for 15 s, annealing, and extension at 60 °C for 60 s according to the manufacturer's instructions. The β-actin was used for the normalization of qPCR data and showed no detectable relative fold change at various tested points and groups. The relative gene expression was calculated by the $2^{-\Delta\Delta Ct}$ method and reported as a relative fold-change over the respective control values. Five alkali injured corneas and five naïve corneas from each group were used for qRT-PCR, each sample was tested in triplicate, and the average fold changes in mRNA levels were reported.

2.8. Rescue experiments with AAV5-DCN gene therapy

To provide the evidence of whether the challenge phenotype (aggravated CNV) is a direct result of the specific *DCN* gene knockout, we have performed a rescue experiment with targeted AAV5-*DCN* gene delivery into alkali injured $Dcn^{-/-}$ mice corneas (n = 10) using custom made cloning cylinder following our earlier published protocol (Mohan et

al., 2011a). The CNV progression in live animals was assessed with stereomicroscope and quantified using an Image J software.

2.9. Statistical analysis

The data were expressed as mean ± SEM. One-way analysis of variance (ANOVA) with Bonferroni post hoc test were used for statistical analysis. GraphPad Prism 9 (GraphPad Software, La Jolla, CA) software was used for statistical analysis and $p \leq 0.05$ was used as the level of significance in different experiments.

3. Results

3.1. Decorin gene deficiency results in aggravated corneal neovascularization

Age- and sex-matched *Dcn*$^{-/-}$ and *Dcn*$^{+/+}$ mice corneas were subjected to alkali injury to study the functional role of the *Dcn* in corneal neovascularization *in vivo*. The severity of corneal neovascularization in live animals was assessed at various time-points up to day 21 post-alkali injury using stereomicroscopic examination (Fig. 1). In a subjective evaluation, *Dcn*$^{-/-}$ mice corneas exhibited aggravated CNV features (area, length, thickness, and density of blood vessels) (Fig. 1D) compared to *Dcn*$^{+/+}$ mice corneas at day-21 post-alkali injury (Fig. 1B). No corneal transparency defects were observed in *Dcn*$^{-/-}$ mice naïve corneas (Fig. 1C) compared to *Dcn*$^{+/+}$ mice naïve corneas (Fig. 1A). Image J analysis showed significantly increased area of blood vessels in alkali injured *Dcn*$^{-/-}$ mice corneas (1.7 fold; $p < 0.05$) than in *Dcn*$^{+/+}$ mice corneas. In rescue experiments, AAV5-*Dcn* gene delivered corneas showed significantly reduced area of blood vessels (2 fold; $p < 0.001$) than the controls (no AAV5-*Dcn* gene delivery) in *Dcn*$^{-/-}$ mice alkali injured corneas (Fig. 2).

3.2. Decorin gene deficiency results in increased structural alterations in alkali injured corneal stroma

To study the morphological changes in corneal tissues, *Dcn*$^{-/-}$ and *Dcn*$^{+/+}$ naïve and day 21 post-alkali injury mice corneal tissue sections were subjected to H&E staining (Fig. 3). No structural changes were observed in *Dcn*$^{-/-}$ mice naïve corneas (Fig. 3C) compared to *Dcn*$^{+/+}$ mice naïve corneas (Fig. 3A). However, *Dcn*$^{-/-}$ mice day 21 post-alkali injury corneal tissue sections showed increased stromal cellular infiltration and distorted collagen lamellae (Fig. 3D) compared to *Dcn*$^{+/+}$ mice day 21 post-alkali injury corneal tissue sections (Fig. 3B).

3.3. Decorin gene deficiency interrupts homeostasis between pro- and anti-angiogenic factors in the cornea

3.3.1. Decorin gene deficiency causes upregulation of pro-angiogenic factors in the cornea—In order to test the hypothesis that *Dcn* maintains the physiologic balance between the pro- and anti-angiogenic factors during corneal angiogenesis, expression of pro- and anti-angiogenic factors in *Dcn*$^{-/-}$ and *Dcn*$^{+/+}$ mice naïve and neovascularized (day 21 post-alkali injury) corneal tissues were assessed using immunofluorescence staining (Fig. 4 and Fig. 5) and qRT-PCR (Fig. 6 and Fig. 7). Immunofluorescence staining demonstrated a significant increase in expression of the pro-angiogenic protein endoglin (Fig. 4) and α-SMA (Fig. 5) in day 21 post- alkali injury

neovascularized corneal tissues compared to naïve corneal tissues in both the $Dcn^{-/-}$ ($p < 0.001$) and $Dcn^{+/+}$ mice ($p < 0.05$). However, $Dcn^{-/-}$ mice neovascularized corneal tissues showed significantly increased expression of endoglin (Fig. 4D) and α-SMA protein (Fig. 5D) compared to $Dcn^{+/+}$ mice neovascularized corneal tissues at day 21 post-alkali injury ($p < 0.05$) (Figs. 4B and 5B).

In the qRT-PCR analysis, $Dcn^{-/-}$ mice naïve corneas showed increased mRNA levels of pro-angiogenic factors *endoglin* (2.53-fold; $p < 0.05$), *Pdgf* (1.33-fold; $p > 0.05$), *Pecam* (2.14-fold; $p < 0.05$), and *Vegf* (2.47 fold; $p < 0.05$) compared to $Dcn^{+/+}$ mice naïve corneas (Fig. 6A–D). In $Dcn^{-/-}$ mice, day 21 post-alkali injury neovascularized corneas showed significantly increased mRNA levels of *endoglin* (4.08- fold; $p < 0.0001$), *Pdgf* (4.86-fold; $p < 0.0001$) and *Vegf* (4.82-fold; $p < 0.0001$) compared to $Dcn^{-/-}$ mice naïve corneas (Fig. 6A, B and D). However, no significant change was observed in expression of *Pecam* in neovascularized $Dcn^{-/-}$ mice corneas compared to naïve corneas (Fig. 6C). In $Dcn^{+/+}$ mice, neovascularized corneas showed increased mRNA levels of *endoglin* (2.22-fold; $p < 0.05$), *Pdgf* (2.88-fold; $p < 0.05$), *Pecam* (2.61-fold; $p < 0.01$), and *Vegf* (3.32-fold; $p < 0.05$) compared to $Dcn^{+/+}$ mice naïve corneas (Fig. 6A–D). $Dcn^{-/-}$ neovascularized mice corneas showed significant upregulation of *endoglin* (4.58 fold; $p < 0.0001$), *Pdgf* (2.15 fold; $p < 0.0001$), and *Vegf* (4.16 fold; $p < 0.0001$) mRNA levels compared to $Dcn^{+/+}$ neovascularized mice corneas (Fig. 6A, B and D). However, no significant change was observed in expression of *Pecam* in neovascularized $Dcn^{-/-}$ mice corneas compared to $Dcn^{+/+}$ neovascularized mice corneas (Fig. 6C).

3.3.2. Decorin gene deficiency causes down-regulation of anti-angiogenic factors during corneal neovascularization—In the qRT-PCR analysis, $Dcn^{-/-}$ mice naïve corneas showed significantly increased mRNA levels of anti-angiogenic factor *Vegfr2* (1.56- fold; $p < 0.05$) (Fig. 7C), and no significant changes ($p > 0.05$) in *Ang2* (1.27-fold), and *Timp1* (1.14-fold) compared to $Dcn^{+/+}$ mice naïve corneas (Fig. 7A–B). In $Dcn^{-/-}$ mice, day 21 post-alkali injury corneas showed significantly decreased mRNA levels of *Ang2* (0.06-fold; $p < 0.0001$), *Timp1* (0.15-fold, $p < 0.001$) and *VegfrR2* (0.11-fold; $p < 0.0001$) compared to $Dcn^{-/-}$ naïve corneas (Fig. 7A–C). In $Dcn^{+/+}$ mice, day 21 post-alkali injury corneas showed decreased mRNA levels of anti- angiogenic factors *Ang2* (0.63-fold; $p < 0.05$), *Timp1* (0.77-fold; $p > 0.05$) and *Vegfr2* (0.26-fold; $p < 0.01$) when compared to naïve corneas (Fig. 7A–C). $Dcn^{-/-}$ mice day 21 post-alkali injury corneal tissues showed decreased mRNA levels of *Ang2* (0.12-fold; $p < 0.05$), *Timp1* (0.22-fold; $p < 0.05$), and *Vegfr2* (0.67-fold; $p > 0.05$) compared to $Dcn^{+/+}$ mice day 21 post-alkali injury corneal tissues (Fig. 7A–C).

4. Discussion

Decorin is a multifunctional proteoglycan that regulates various cellular processes including angiogenesis, fibrosis, autophagy, diabetic nephropathy, myocardial infarct, inflammation, innate immunity, and wound healing (Gubbiotti et al., 2016; Järveläinen et al., 2015; Neill et al., 2012). In a healthy cornea, DCN plays a key role in maintaining corneal transparency by exerting its anti-fibrotic and anti-angiogenic properties. However, tissue injury leads to imbalanced corneal homeostasis and causes fibrosis and angiogenesis to occur (Mohan

et al., 2011a, b,c). Corneal injury induces the secretion of Matrix metalloproteinases (MMPs), a family of highly homologous zinc endopeptidases that degrade the corneal basement membrane, cleave DCN and promote corneal angiogenesis. Mimura et al. reported the upregulation of MT-MMP1 in vascularized corneas which can cleave DCN in a concentration and time-dependent manner (Mimura et al., 2009). In our earlier report, overexpression of DCN via AAV-*Dcn* gene therapy into the corneal stroma significantly reduced the development of corneal angiogenesis (Mohan et al., 2011a,b,c). In the current report, we demonstrate the functional role of DCN in corneal transparency by maintaining homeostasis between pro-and anti-angiogenic factors using *Dcn* deficient mice.

Dcn deficiency in knockout mice results in distinct phenotypes in various connective tissues. *Dcn* gene knockout mice showed alterations in collagen fibrillogenesis, and collagen morphology in skin and tendon which leads to reduced tensile strength, fragile skin and abnormal tendon phenotype (Danielson et al., 1997). Schönherr et al., reported a reduced angiogenic response in *Dcn* deficient mice injured corneas compared to wildtype mice corneas (Schönherr et al., 2004). In our study, *Dcn* deletion did not affect the structure and transparency of the naïve cornea (Figs. 1C, 2A and 3C) and these results are not surprising that another small leucine-rich proteoglycan biglycan gene expression was reported to be up-regulated in *Dcn* deficient mice cornea to compensate for the role of *Dcn* (Zang et al., 2009). However, *Dcn* gene deletion showed increased neovascularization (Fig. 1D), cellular infiltration, and stromal distortion (Fig. 3D) in day 21 post-alkali injury corneas compared to $Dcn^{+/+}$ mice day 21 post-alkali injury corneas. These results suggest that the abnormalities in the *Dcn* gene function may lead to increased susceptibility to CNV against corneal insult and further ultrastructural studies are warrened to understand how the *Dcn* gene deficiency leads to fibrillar structural alterations and increased CNV response in injured cornea. However, our study results are in contrast to the Schonherr et al., study results (Schönherr et al., 2004) and the discrepancies between these two studies could be due to differences in the methodology used for CNV induction and the time points used to evaluate the CNV response. In Schonherr et al., study, a silver nitrate applicator stick was placed onto the center of the cornea for 1 s to create a 1 mm diameter wound on both the corneas, and the CNV response was monitored up to 72 h (Schönherr et al., 2004). In our study, a 2 mm diameter wound was created by placing a filter paper disc presoaked in NaOH onto the center of the cornea for 30 s, and CNV response was monitored for up to 21 days. These results suggest that *Dcn* can acts as pro-angiogenic or anti-angiogenic molecule depending on the cellular and molecular microenvironment and the angiogenic stimuli.

In the cornea, DCN functions mainly through interaction with different growth factors and cell surface receptors. VEGF is a key regulatory factor for corneal angiogenesis and its expression is upregulated in corneal pathologies, such as injury, inflammation, and infections (Roshandel et al., 2018). The angiogenic activity of VEGF is through binding with VEGFR2, and the interaction of VEGF with VEGFR2 activates angiogenic cascades that lead to the formation of new blood vessels (Roshandel et al., 2018). Epithelial, stromal, and endothelial cells are the main sources of VEGF in the cornea (Roshandel et al., 2018). In the naïve cornea, the basement membrane sequesters the VEGF secreted from the epithelium (Van Setten, 1997), and in the stroma, DCN binds to VEGF and inhibits or reduces its bioavailability and activity (Järveläinen et al., 2015). Endoglin is a pro-angiogenic

molecule and its expression levels are upregulated in angiogenesis. Endoglin promotes VEGF-induced endothelial tip cell formation via its interaction with VEGFR2 (Tian et al., 2018). *Dcn*$^{-/-}$ mice naïve and neovascularized corneas showed increased upregulation of *Vegf* and *endoglin* compared to *Dcn*$^{+/+}$ mice naïve and neovascularized corneas, respectively (Fig. 6A and D). However, the association of DCN with endoglin is not known.

Endothelial cells and pericytes are the two principal cell types of typical angiogenic microvessel walls. Endothelial cells form the vascular tube inner lining, and pericytes form an outer sheath around the endothelia. PDGF recruits pericytes to angiogenic vessels, and interaction of PDGF with its receptor PDGFR stimulates pericyte proliferation (Chaoran et al., 2011). DCN also interacts with the angiogenic growth factor PDGF and prevents its bioactivity via inhibition of PDGFR phosphorylation (Nili et al., 2003). *Dcn*$^{-/-}$ mice neovascularized corneas showed significantly higher expression of *Pdgf* than *Dcn*$^{+/+}$ neovascularized corneas (Fig. 6B).

PECAM, a pro-angiogenic molecule expressed on endothelial cells (ECs), is a transmembrane glycoprotein member of the Ig superfamily that promotes endothelial cell migration in angiogenesis via the formation of filopodia (Cao et al., 2009). In this study, *Dcn*$^{-/-}$ mice naïve cornea showed significantly more upregulation of *Pecam* than *Dcn*+/+ naïve corneas (Fig. 6C). In *Dcn*$^{+/+}$ mice, *Pecam* expression was significantly upregulated in the neovascularized corneas compared to naïve corneas (Fig. 6C). However, in *Dcn*$^{-/-}$ mice, *Pecam* expression was not changed in the neovascularized corneas as compared to naïve corneas (Fig. 6C), and the association of DCN with PECAM is not known.

DCN core protein has two binding sites for TGF-β, a cytokine known for its role in regulating both immune and stem cells. The interaction between DCN and TGF-β prevents the binding of TGF-β to its receptors and inhibits TGF-β dependent signaling, α-SMA expression, and fibrosis (Gubbiotti et al., 2016; Mohan et al., 2011a,b,c). In *Dcn*$^{-/-}$ mice, neovascularized corneas showed significantly increased expression of α-SMA protein compared to neovascularized *Dcn*$^{+/+}$ corneas (Fig. 3).

Ang2 is a natural antagonist for Ang1 and Tie2. Ang2 is an anti-angiogenic factor, and transgenic overexpression of Ang2 disrupts the formation of blood vessels in the mouse embryo (Maisonpierre et al., 1997). However, Ang2 also acts as a pro-angiogenic factor and its biological activity is context-dependent (Oshima et al., 2005; Akwii et al., 2019). In a healthy cornea, MMPs and TIMPs regulate ECM structural architecture. During angiogenesis, ECM proteins are cleaved by MMPs. TIMPs act as anti-angiogenic molecules that regulate the proteolytic activities of MMPs by forming inhibitory complexes. TIMP1 inhibits endothelial cell migration and its response to angiogenic factors and blocks chemotaxis (Sang, 1998). DCN is known to stimulate the synthesis of TIMP2 and TIMP3 (Järveläinen et al., 2015). Despite this, adenovirus-mediated overexpression of DCN did not affect TIMP1 expression in cultured human gingival fibroblasts (Al Haj Zen et al., 2003). DCN also has a high affinity with VEGFR2 and their interaction leads to inhibition of VEGFR2 signaling and blocking angiogenesis (Järveläinen et al., 2015). The loss of DCN function showed significant upregulation of *Vegfr2* and no significant impact on the expression of *Ang2*, and *Timp1* in naïve cornea (Fig. 7). However, neovascularized *Dcn*$^{-/-}$

mice corneas showed reduced expression of *Ang2*, *Timp1*, and *Vegfr2* genes compared to *Dcn*$^{-/-}$ mice naïve corneas and *Dcn*$^{+/+}$ mice day 21 post-alkali injury corneas (Fig. 7).

DCN exhibits anti-angiogenic properties by regulating *Vegf* gene acitivty as reported by many investiagors. In a micro-pocket corneal neovascularization mouse model, a decrease in *Vegf* mRNA expression was observed in animals given AAV5-*DCN* gene therapy (Mohan et al., 2011a,b,c). In DCN, the presence of glycosaminoglycan (GAG) chain and specific binding motifs in its protein core influences the bioactivity and availability of several angiogenic growth factors by sequestering growth factors and their interaction with its specific receptors (Gubbiotti et al., 2016). When DCN is deficient in the cornea, there appears to be reduced sequestration of VEGF in the corneal stroma through core protein mechanism and, at least partly, allowing higher VEGF levels in the stroma. We predict that lack of decorin core protein renders upregulation of *Vegf gene* expression by paracrine mechanism and angiogenic response in the cornea (Mohan et al., 2011a,b,c). The *Dcn*$^{-/-}$ mice showed aggravated corneal neovascularization induced by alkali injury compared to *Dcn*$^{+/+}$ mice (Fig. 1).

5. Conclusion

This study results suggest that DCN plays an important role in the maintenance of corneal transparency and wound repair post-injury by influencing the expression of pro- and anti-angiogenic factors.

Acknowledgments

This work was primarily supported by the NEI/NIH R01EY017294, R01EY030774, and U01EY031650 grants (RRM), and partial support from the United States Department of Veterans Health Affairs Merit 1I01BX00357 and Research Career Scientist grants (RRM), and Ruth M. Kraeuchi Missouri Endowed Chair Ophthalmology University of Missouri Fund (RRM).

References

Akwii RG, Sajib MS, Zahra FT, Mikelis CM, 2019. Role of angiopoietin-2 in vascular physiology and pathophysiology. Cells 8, 471. 10.3390/cells8050471.

Al Haj Zen A, Lafont A, Durand E, Brasselet C, Lemarchand P, Godeau G, Gogly B, 2003. Effect of adenovirus-mediated overexpression of decorin on metalloproteinases, tissue inhibitors of metalloproteinases and cytokines secretion by human gingival fibroblasts. Matrix Biol. 22, 251–258. 10.1016/s0945-053x(03)00018-0. [PubMed: 12853035]

Aydin E, Kivilcim M, Peyman GA, Esfahani MR, Kazi AA, Sanders DR, 2008. Inhibition of experimental angiogenesis of cornea by various doses of doxycycline and combination of triamcinolone acetonide with low-molecular-weight heparin and doxycycline. Cornea 27, 446–453. 10.1097/ICO.0b013e3181605ff9. [PubMed: 18434849]

Azar DT, 2006. Corneal angiogenic privilege: angiogenic and antiangiogenic factors in corneal avascularity, vasculogenesis, and wound healing (an American Ophthalmological Society thesis). Trans. Am. Ophthalmol. Soc. 104, 264–302. [PubMed: 17471348]

Bachmann B, Taylor RS, Cursiefen C, 2010. Corneal neovascularization as a risk factor for graft failure and rejection after keratoplasty: an evidence-based meta- analysis. Ophthalmology 117, 1300–1305. 10.1016/j.ophtha.2010.01.039e7 [PubMed: 20605214]

Cao G, Fehrenbach ML, Williams JT, Finklestein JM, Zhu JX, Delisser HM, 2009. Angiogenesis in platelet endothelial cell adhesion molecule-1-null mice. Am. J. Pathol. 175, 903–915. 10.2353/ajpath.2009.090206. [PubMed: 19574426]

Chaoran Z, Zhirong L, Gezhi X, 2011. Combination of vascular endothelial growth factor receptor/platelet-derived growth factor receptor inhibition markedly improves the antiangiogenic efficacy for advanced stage mouse corneal neovascularization. Graefes Arch. Clin. Exp. Ophthalmol. 249, 1493–1501. 10.1007/s00417-011-1709-6. [PubMed: 21574021]

Danielson KG, Baribault H, Holmes DF, et al. , 1997. Targeted disruption of decorin leads to abnormal collagen fibril morphology and skin fragility. J. Cell Biol. 136, 729–743. 10.1083/jcb.136.3.729. [PubMed: 9024701]

Dekaris I, Gabric N, Draca N, et al. , 2015. Three-year corneal graft survival rate in highrisk cases treated with subconjunctival and topical bevacizumab. Graefes Arch. Clin. Exp. Ophthalmol. 253, 287–294. 10.1007/s00417-014-2851-8. [PubMed: 25398659]

Faraj LA, Said DG, Dua HS, 2011. Evaluation of corneal neovascularisation. Br. J. Ophthalmol. 95, 1343–1344. 10.1136/bjophthalmol-2011-300856. [PubMed: 21937569]

Gubbiotti MA, Vallet SD, Ricard-Blum S, Iozzo RV, 2016. Decorin interacting network: a comprehensive analysis of decorin-binding partners and their versatile functions. Matrix Biol. 55, 7–21. 10.1016/j.matbio.2016.09.009. [PubMed: 27693454]

Järveläinen H, Sainio A, Wight TN, 2015. Pivotal role for decorin in angiogenesis. Matrix Biol. 43, 15–26. 10.1016/j.matbio.2015.01.023. [PubMed: 25661523]

Kim TI, Chung JL, Hong JP, et al. , 2009. Bevacizumab application delays epithelial healing in rabbit cornea. Invest. Ophthalmol. Vis. Sci. 50, 4653–4659. 10.1167/iovs.08-2805. [PubMed: 19458331]

Kim EC, Ryu HW, Lee HJ, Kim MS, 2013. Bevacizumab eye drops delay corneal epithelial wound healing and increase the stromal response to epithelial injury in rats. Clin. Exp. Ophthalmol. 41, 694–701. 10.1111/ceo.12085. [PubMed: 23433183]

Kim SJ, Lee JW, Yu SL, et al. , 2013. The role of Nod1 signaling in corneal neovascularization. Cornea 32, 674–679. 10.1097/ICO.0b013e3182781ea4. [PubMed: 23328697]

Kitano A, Okada Y, Yamanka O, et al. , 2010. Therapeutic potential of trichostatin A to control inflammatory and fibrogenic disorders of the ocular surface. Mol. Vis. 2010; 16, 2964–2973.

Lee P, Wang CC, Adamis AP, 1998. Ocular neovascularization: an epidemiologic review. Surv. Ophthalmol. 43, 245–269. 10.1016/s0039-6257(98)00035-6. [PubMed: 9862312]

Lim P, Fuchsluger TA, Jurkunas UV, 2009. Limbal stem cell deficiency and corneal neovascularization. Semin. Ophthalmol. 24, 139–148. 10.1080/08820530902801478. [PubMed: 19437349]

Liu X, Wang S, Wang X, Liang J, Zhang Y, 2017. Recent drug therapies for corneal neovascularization. Chem. Biol. Drug Des. 90, 653–664. 10.1111/cbdd.13018. [PubMed: 28489275]

Maisonpierre PC, Suri C, Jones PF, Bartunkova S, Wiegand SJ, Radziejewski C, Compton D, McClain J, Aldrich TH, Papadopoulos N, Daly TJ, Davis S, Sato TN, Yancopoulos GD, 1997. Angiopoietin-2, a natural antagonist for Tie2 that disrupts in vivo angiogenesis. Science 277, 55–60. 10.1126/science.277.5322.55. [PubMed: 9204896]

Mimura T, Han KY, Onguchi T, Chang JH, Kim TI, Kojima T, Zhou Z, Azar DT, 2009. MT1-MMP-mediated cleavage of decorin in corneal angiogenesis. J. Vasc. Res. 46, 541–550. 10.1159/000226222. [PubMed: 19571574]

Mohan RR, Stapleton WM, Sinha S, Netto MV, Wilson SE, 2008. A novel method for generating corneal haze in anterior stroma of the mouse eye with the excimer laser. Exp. Eye Res. 86, 235–240. [PubMed: 18068702]

Mohan RR, Tovey JCK, Sharma A, Schultz GS, Cowden JW, et al. , 2011a. Targeted decorin gene therapy delivered with adeno-associated virus effectively retards corneal neovascularization in vivo. PloS One 6, e26432. 10.1371/journal.pone.0026432.

Mohan RR, Tovey JCK, Gupta R, Sharma A, Tandon A, 2011b. Decorin biology, expression, function and therapy in the cornea. Curr. Mol. Med. 11, 110–128. 10.2174/156652411794859241. [PubMed: 21342131]

Mohan RR, Tandon A, Sharma A, Cowden JW, Tovey JC, 2011c. Significant inhibition of corneal scarring in vivo with tissue-selective, targeted AAV5 decorin gene therapy. Invest. Ophthalmol. Vis. Sci. 52, 4833–4841. 10.1167/iovs.11-7357. [PubMed: 21551414]

Neill T, Painter H, Buraschi S, et al. , 2012. Decorin Antagonizes the Angiogenic Network. Concurrent inhibition of Met, hypoxia inducible factor-1α and vascular endothelial growth factor A and induction of thrombospondin-1 and TIMP3. J. Biol. Chem. 287, 5492–5506. 10.1074/jbc.M111.283499. [PubMed: 22194599]

Nili N, Cheema AN, Giordano FJ, et al. , 2003. Decorin inhibition of PDGF- stimulated vascular smooth muscle cell function: potential mechanism for inhibition of intimal hyperplasia after balloon angioplasty. Am. J. Pathol. 163, 869–878. 10.1016/S0002-9440(10)63447-5. [PubMed: 12937128]

Oshima Y, Oshima S, Nambu H, et al. , 2005. Different effects of angiopoietin-2 in different vascular beds: new vessels are most sensitive. Faseb. J. 19, 963–965. 10.1096/fj.04-2209fje. [PubMed: 15802489]

Papathanassiou M, Theodoropoulou S, Analitis A, et al. , 2013. Vascular endothelial growth factor inhibitors for treatment of corneal neovascularization: a metaanalysis. Cornea 2013; 32, 435–444. 10.1097/ICO.0b013e3182542613.

Petsoglou C, Balaggan KS, Dart JK, et al. , 2013. Subconjunctival bevacizumab induces regression of corneal neovascularisation: a pilot randomised placebo- controlled double-masked trial. Br. J. Ophthalmol. 97, 28–32. 10.1136/bjophthalmol-2012-302137. [PubMed: 23087419]

Roshandel D, Eslani M, Baradaran-Rafii A, et al. , 2018. Current and emerging therapies for corneal neovascularization. Ocul. Surf. 16, 398–414. [PubMed: 29908870]

Sang QX, 1998. Complex role of matrix metalloproteinases in angiogenesis. Cell Res. 8, 171–177. 10.1038/cr.1998.17. [PubMed: 9791730]

Schneider CA, Rasband WS, Eliceiri KW, 2012. NIH Image to ImageJ: 25 years of image analysis. Nat. Methods 9, 671–675. [PubMed: 22930834]

Schonherr E, Sunderkötter C, Schaefer L, et al. , 2004. Decorin deficiency leads to impaired angiogenesis in injured mouse cornea. J. Vasc. Res. 41, 499–508. 10.1159/000081806. [PubMed: 15528932]

Shi W, Liu J, Li M, et al. , 2010. Expression of MMP, HPSE, and FAP in stroma promoted corneal neovascularization induced by different etiological factors. Curr. Eye Res. 35, 967–977. 10.3109/02713683.2010.502294. [PubMed: 20958185]

Tian H, Huang JJ, Golzio C, Gao X, Hector-Greene M, Katsanis N, Blobe GC, 2018. Endoglin interacts with VEGFR2 to promote angiogenesis. Faseb. J. 32, 2934–2949. 10.1096/fj.201700867RR. [PubMed: 29401587]

Tripathi R, Giuliano EA, Gafen HB, Gupta S, Martin LM, Sinha PR, Rodier JT, Fink MK, Hesemann NP, Chaurasia SS, Mohan RR, 2019. Is sex a biological variable in corneal wound healing? Exp. Eye Res. 187, 107705 10.1016/j.exer.2019.107705.

Van Setten GB, 1997. Vascular endothelial growth factor (VEGF) in normal human corneal epithelium: detection and physiological importance. Acta Ophthalmol. Scand. 75, 649–652. 10.1111/j.1600-0420.1997.tb00623.x. [PubMed: 9527324]

Wang Z, Cheng R, Lee K, et al. , 2015. Nanoparticle-mediated expression of a Wnt pathway inhibitor ameliorates ocular neovascularization. Arterioscler. Thromb. Vasc. Biol. 35, 855–864. 10.1161/ATVBAHA.114.304627. [PubMed: 25657312]

Yin L, Morishige K, Takahashi T, et al. , 2007. Fasudil inhibits vascular endothelial growth factor-induced angiogenesis in vitro and in vivo. Mol. Canc. Therapeut. 6, 1517–1525. 10.1158/1535-7163.MCT-06-0689.

Zhang G, Chen S, Goldoni S, et al. , 2009. Genetic evidence for the coordinated regulation of collagen fibrisllogenesis in the cornea by decorin and biglycan. J. Biol. Chem. 284, 8888–8897. 10.1074/jbc.M806590200. [PubMed: 19136671]

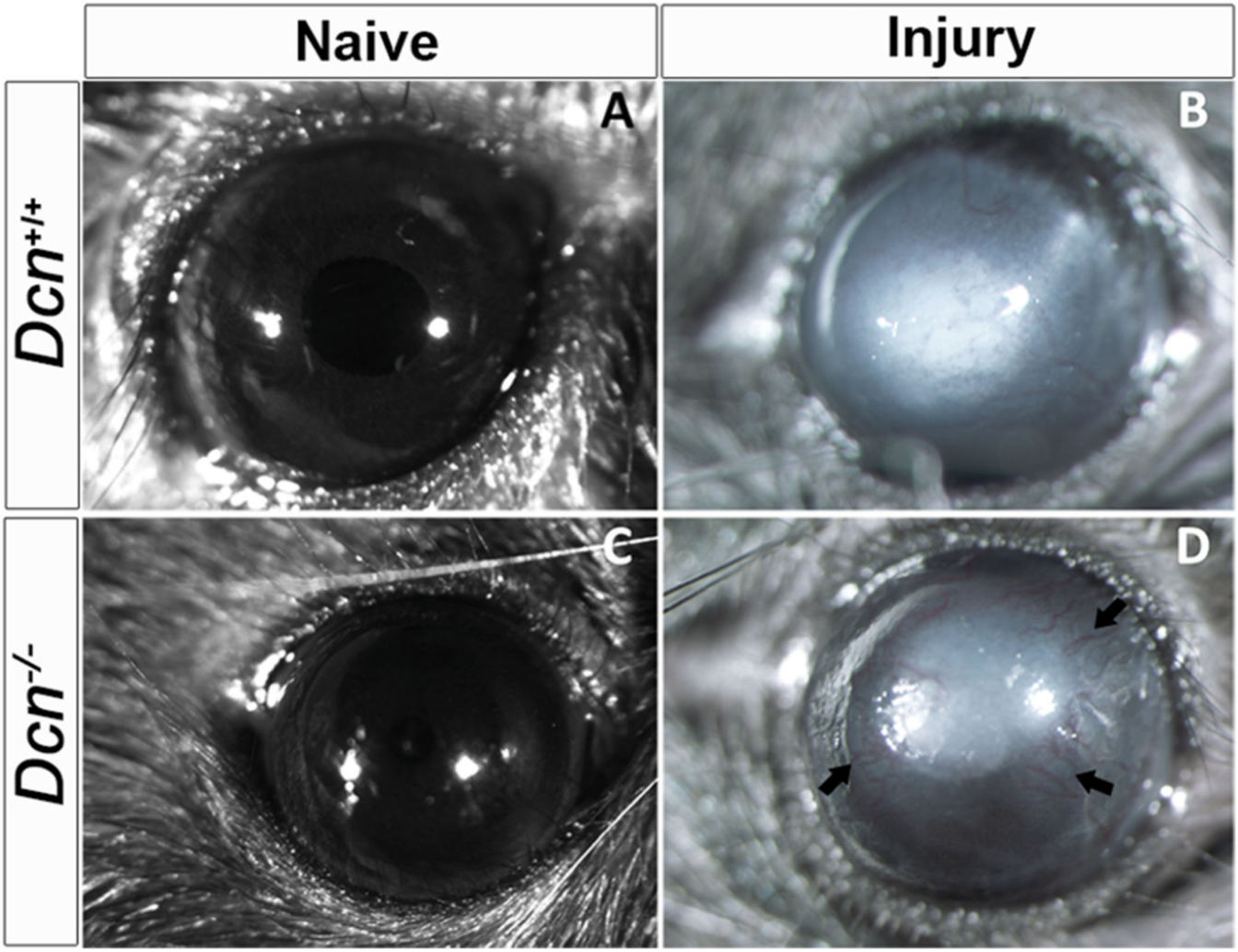

Fig. 1.

Representative stereo-microscopic images of wild type (*Dcn* $^{+/+}$) mice and *Dcn* $^{-/-}$ mice corneas before alkali injury and 21 days post-alkali injury (n = 10 in each group). Increased corneal neovascularization was observed in *Dcn* $^{-/-}$ mice (D) compared to *Dcn* $^{+/+}$ mice (B) at day 21 post-alkali injury. (A and C) Naïve corneas of *Dcn* $^{+/+}$ and *Dcn* $^{-/-}$ mice, respectively.

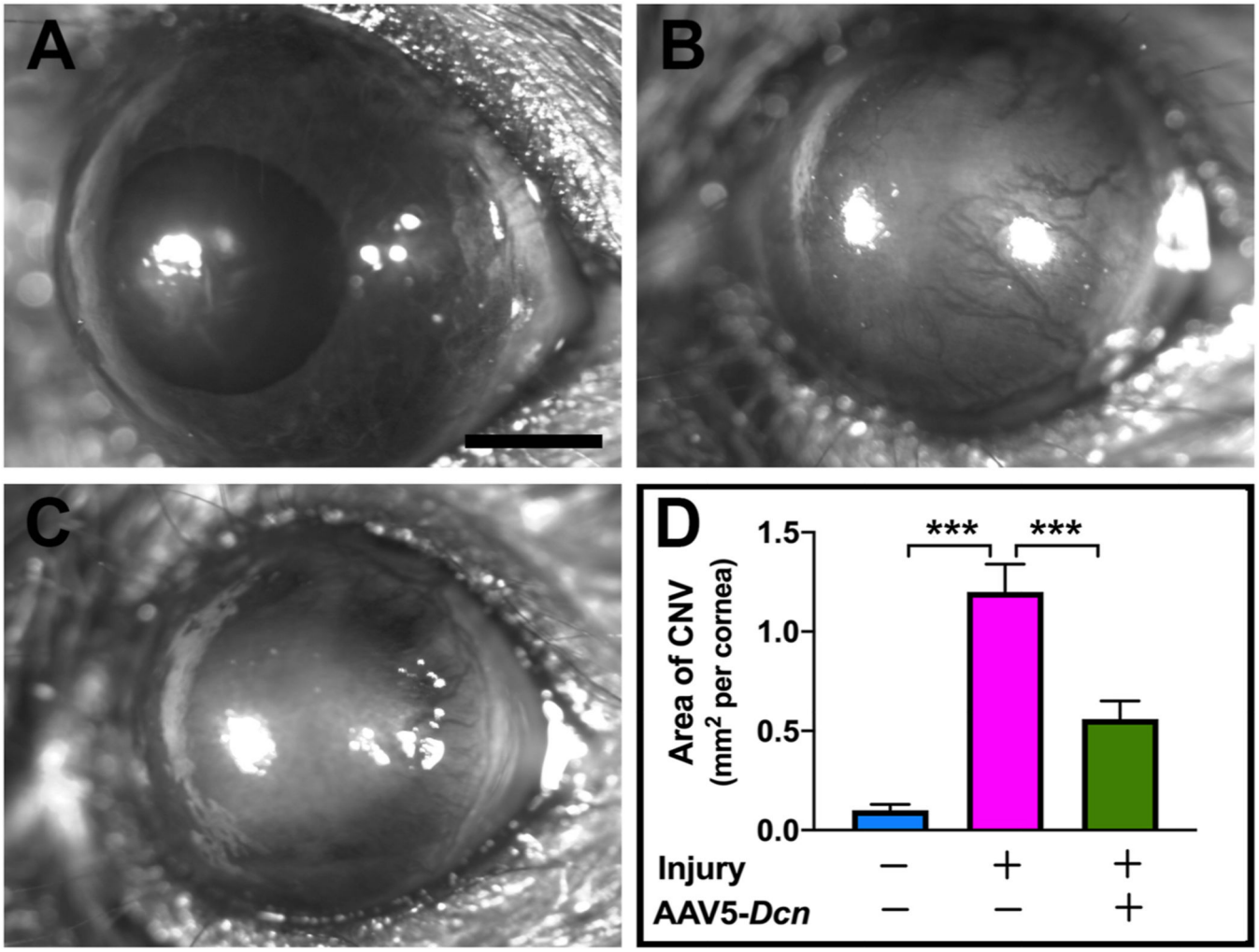

Fig. 2.

Representative stereo-microscopic images of *Dcn* $^{-/-}$ mice naïve corneas (A) and alkali injured untreated corneas (B) and alkali injured corneas treated with AAV5-*Dcn* gene therapy (C) at 21 days post-injury (n = 10 in each group). AAV5-*Dcn* gene therapy significantly reduced corneal neovascularization in *Dcn* $^{-/-}$ mice alkali injured corneas (C and D) compared no therapy group (B and D) at day 21 post-alkali injury. (One-Way ANOVA, ***$p < 0.001$, scale bar = 0.5 mm).

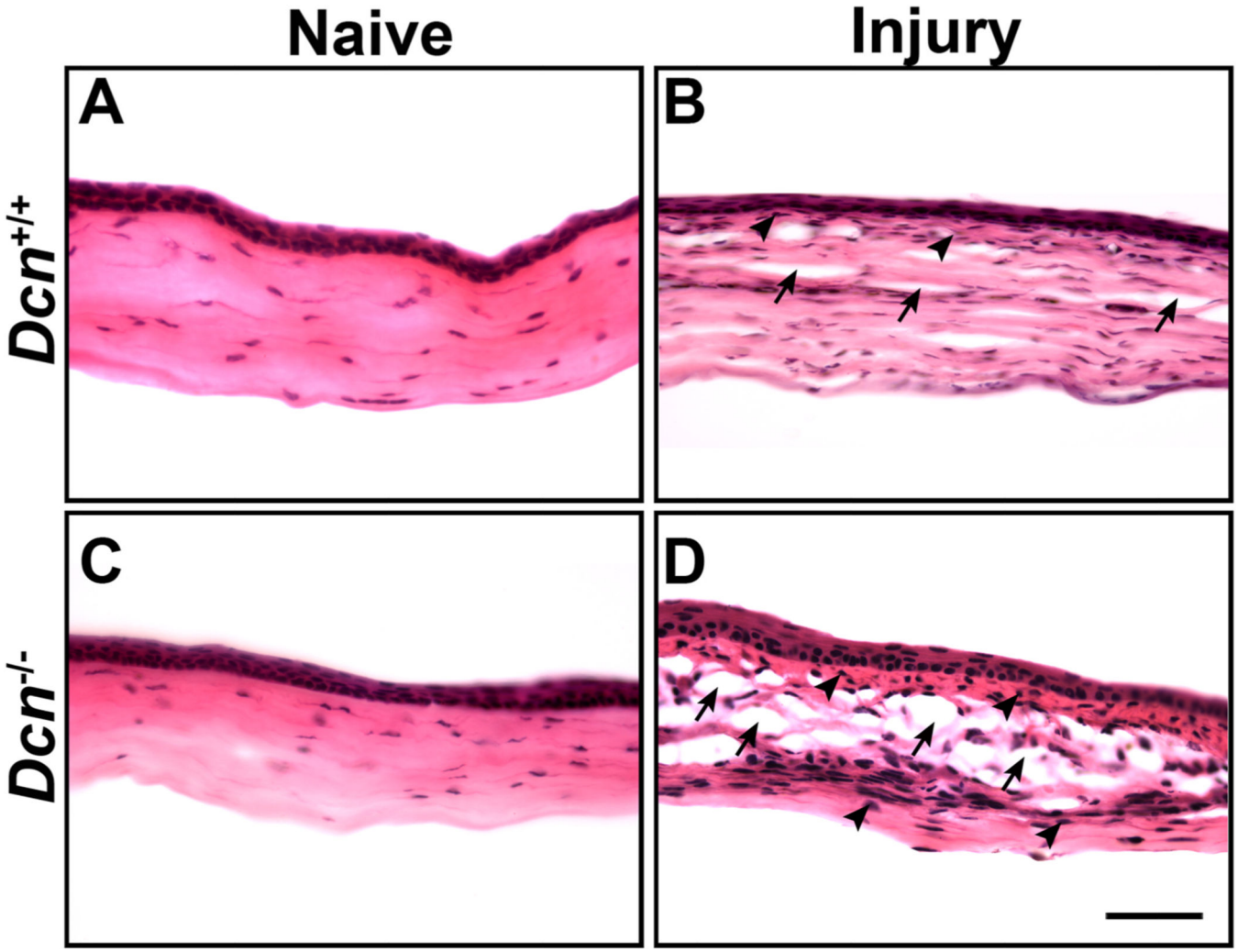

Fig. 3.

Representative images of H & E staining showing the morphological changes in wild type (*Dcn*$^{+/+}$) mice and *Dcn*$^{-/-}$ mice naïve and neovascularized corneas at day 21 post-alkali injury (n = 5 in each group). In a subjective evaluation, no structural changes were observed in *Dcn*$^{+/+}$ *vs. Dcn*$^{-/-}$ mice naïve corneas (A and C). An increased cellular infiltration (indicated by arrowheads) and distorted collagen lamellae (indicated by arrows) were observed in the corneal stroma of *Dcn*$^{-/-}$ mice (D) compared to *Dcn*$^{+/+}$ mice (B) at day 21 post-alkali injury. Scale bar = 50 μm.

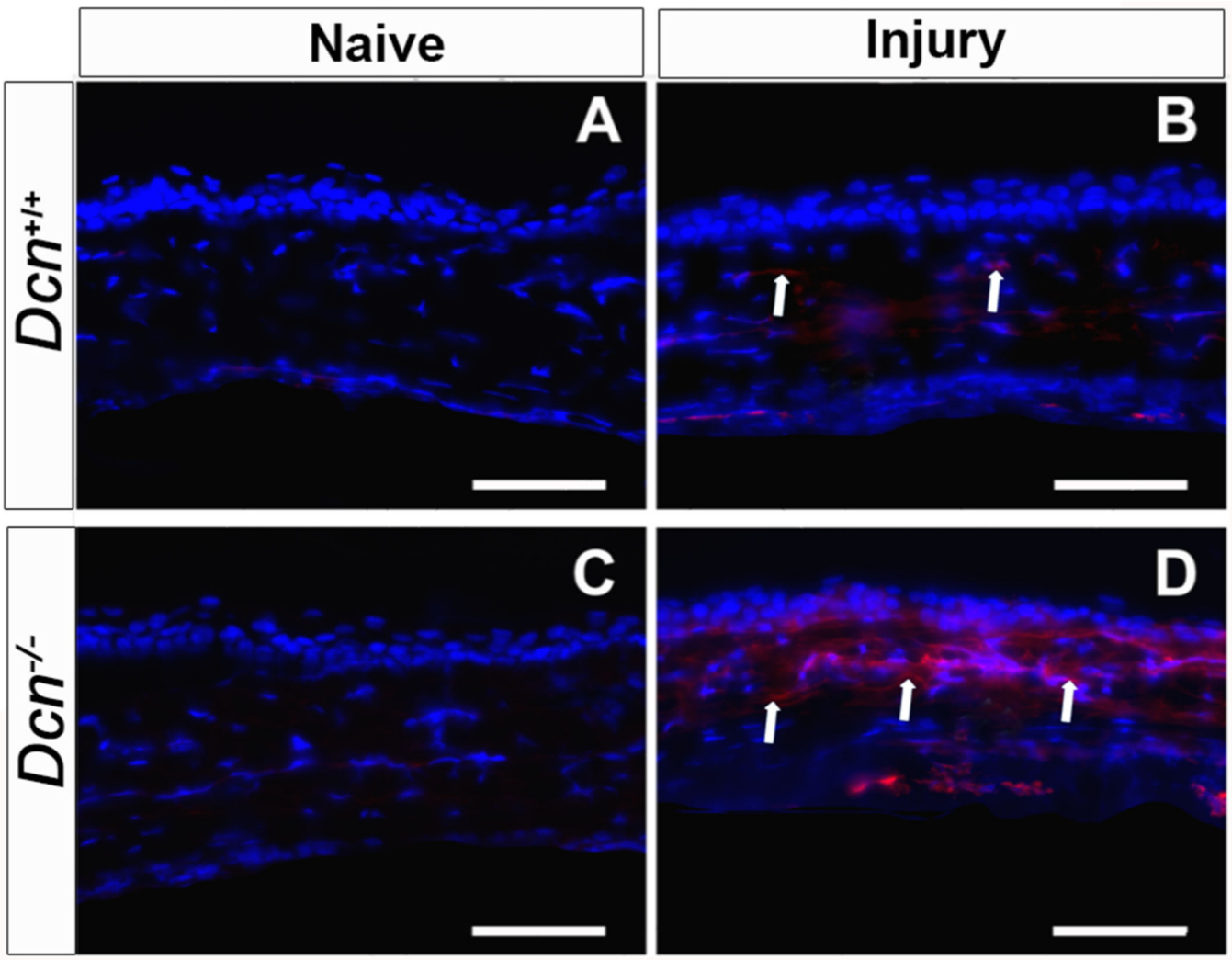

Fig. 4.

Representative immunofluorescence staining images showing expression of angiogenic protein endoglin in wild type (*Dcn*$^{+/+}$) mice and *Dcn*$^{-/-}$ mice naïve and neovascularized corneas at day 21 post- alkali injury (n = 5 in each group). Increased expression of Endoglin (indicated by arrows) was observed in alkali injury- induced *Dcn*$^{-/-}$ mice neovascularized cornea (D) than wild type (*Dcn*$^{+/+}$) mice neovascularized cornea (B) at day-21 post- injury. No endoglin positive cell was observed in the naïve cornea of *Dcn*$^{+/+}$ (A) and *Dcn*$^{-/-}$ mice (C). Scale bar = 50 μm.

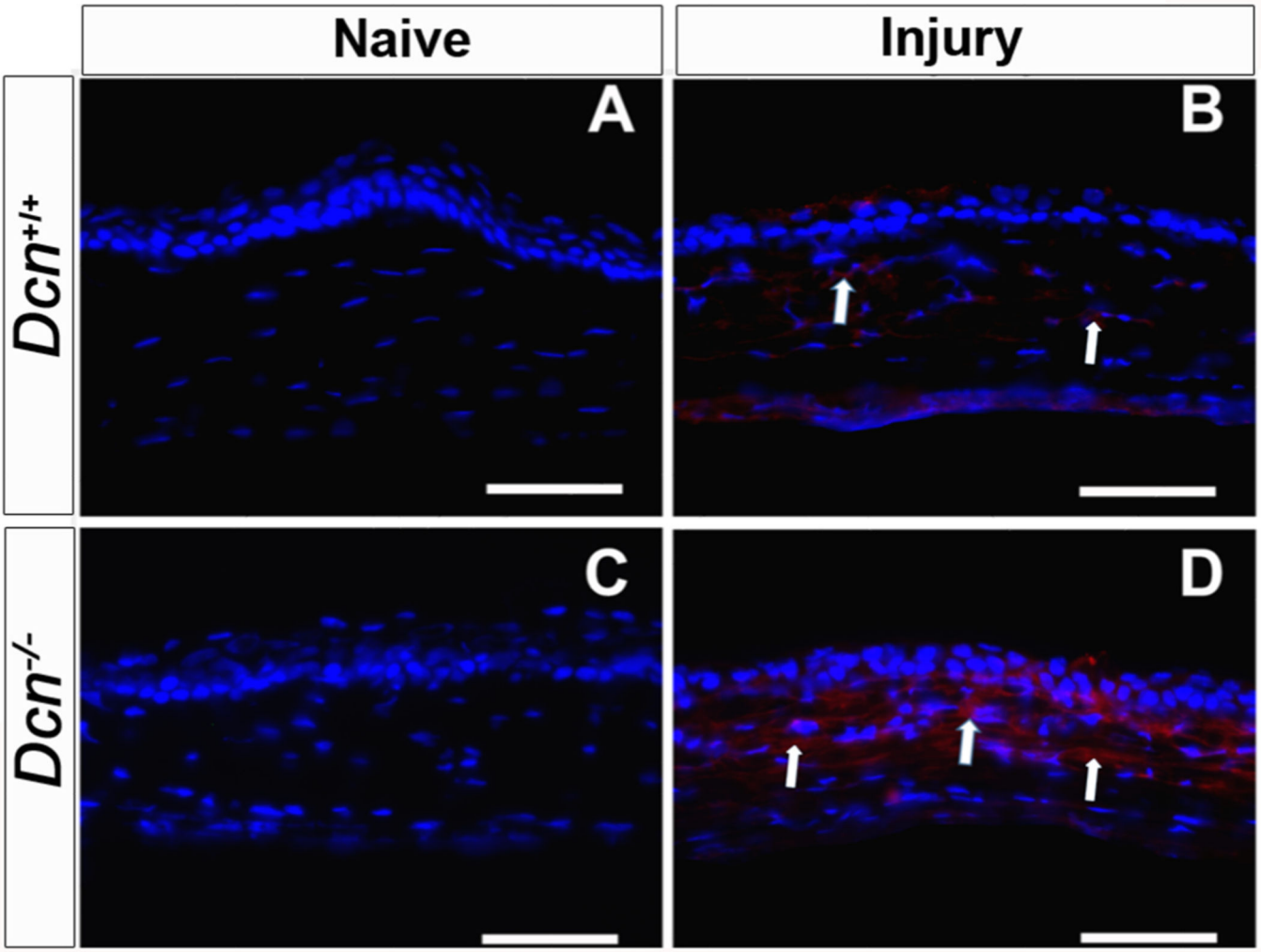

Fig. 5.

Representative immunofluorescence staining images showing expression of α-SMA in wild type (*Dcn*$^{+/+}$) mice and *Dcn*$^{-/-}$ mice naïve and neovascularized corneas at day 21 post-alkali injury (n = 5 in each group). Increased expression of angiogenic protein α-SMA (indicated by arrows) in alkali injury-induced *Dcn*$^{-/-}$ mice neovascularized cornea (D) than wild type (*Dcn*$^{+/+}$) mice neovascularized cornea (B) (at day 21 post-injury). No α-SMA positive cell was observed in the naïve cornea of *Dcn*$^{+/+}$ (A) and *Dcn*$^{-/-}$ mice (C). Scale bar = 50 μm.

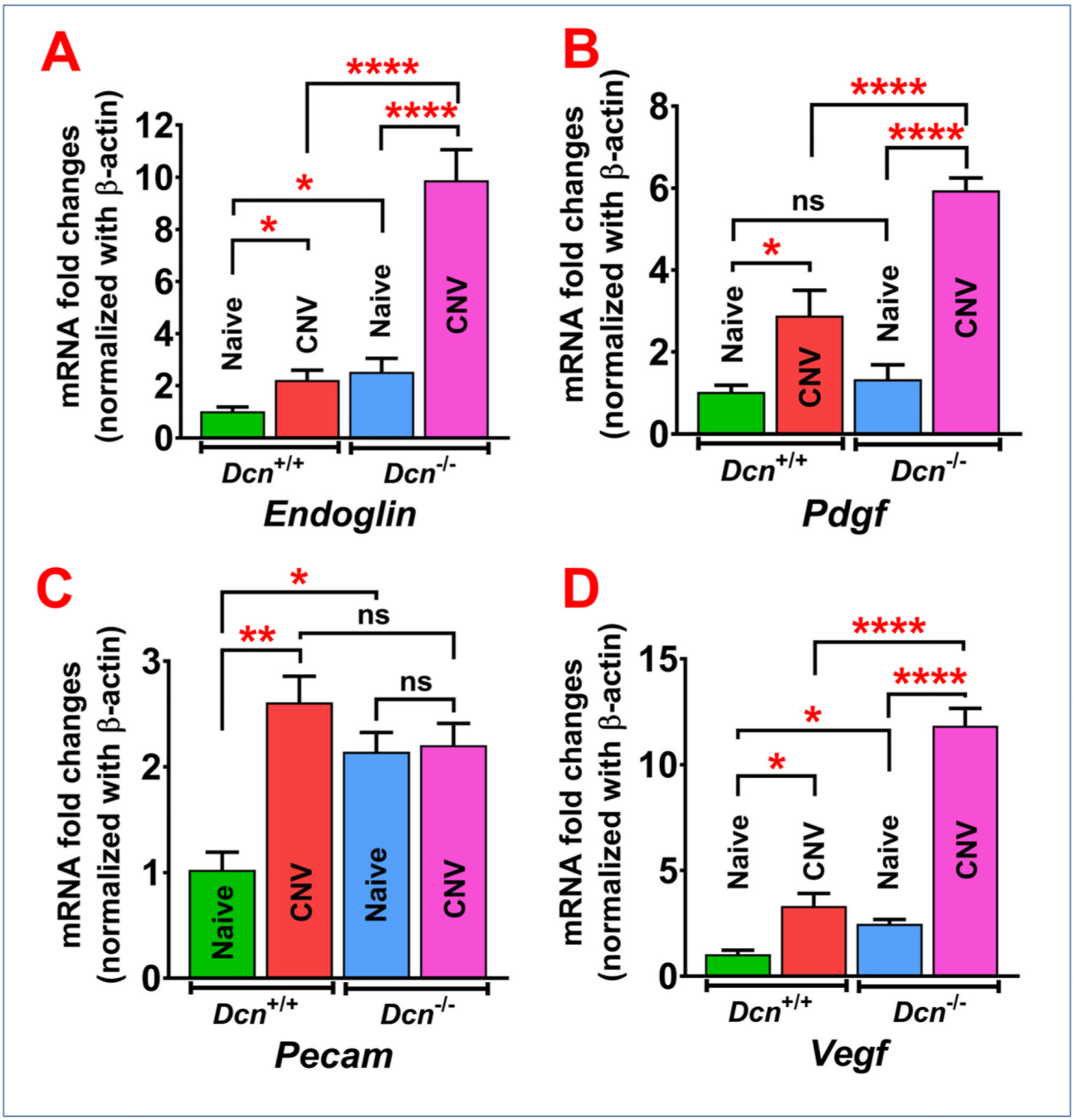

Fig. 6.

qRT-PCR results showing expression of pro-angiogenic genes in wild type (*Dcn*$^{+/+}$) mice and *Dcn*$^{-/-}$ mice naïve and neovascularized corneas at day 21 post-alkali injury (n = 5 in each group). Significant upregulation of pro-angiogenic genes (A) *endoglin and* (D) *Vegf* mRNA expression was observed in neovascularized corneas *vs* naïve corneas in both the *Dcn*$^{+/+}$ and *Dcn*$^{-/-}$ mice and naïve and neovascularized corneas of *Dcn*$^{+/+}$ mice *vs Dcn*$^{-/-}$ mice. (B) *Pdgf* mRNA expression was significantly upregulated in neovascularized corneas *vs* naïve corneas in both the *Dcn*$^{+/+}$ and *Dcn*$^{-/-}$ mice and neovascularized corneas of *Dcn*$^{+/+}$

mice *vs* *Dcn*$^{-/-}$ mice. (C) *Pecam* mRNA expression was significantly upregulated in *Dcn*$^{+/+}$ mice neovascularized corneas *vs* naïve corneas and in naïve corneas of *Dcn*$^{-/-}$ mice *vs* *Dcn*$^{+/+}$ mice. Results are expressed as mean ± SEM (One-Way ANOVA, *$p < 0.05$, **$p < 0.01$, and ****$p < 0.0001$).

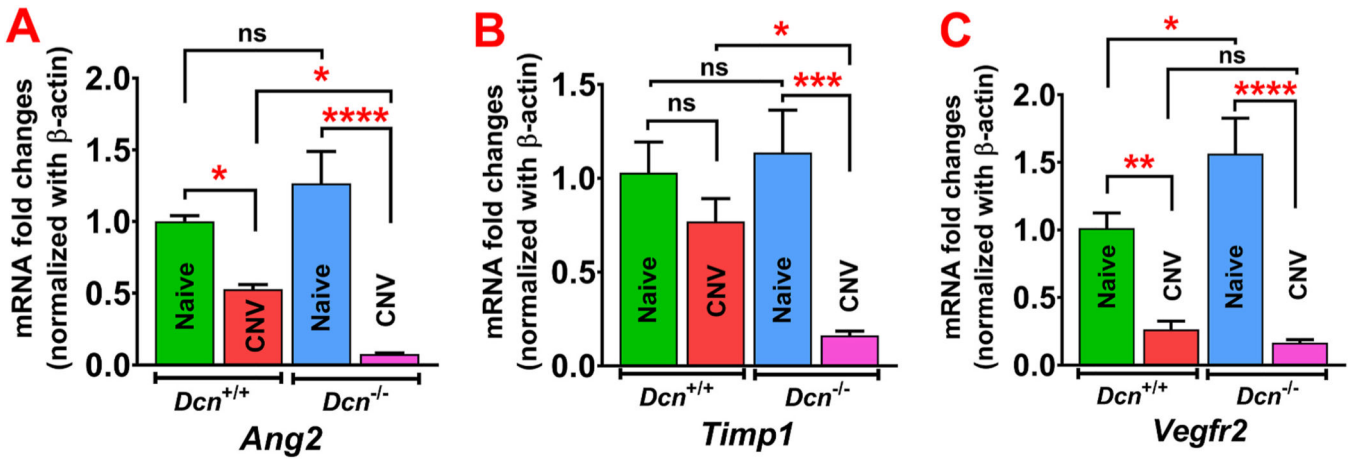

Fig. 7.

qRT-PCR results showing expression of anti-angiogenic genes in wild type (*Dcn*$^{+/+}$) mice and *Dcn*$^{-/-}$ mice naïve and neovascularized corneas at day 21 post- alkali injury (n = 5 in each group). (A) Significant reduction in anti-angiogenic gene *Ang2* mRNA expression was observed in neovascularized corneas *vs* naïve corneas in both the *Dcn*$^{+/+}$ and *Dcn*$^{-/-}$ mice. Neovascularized *Dcn*$^{-/-}$ mice corneas showed a significant reduction of *Ang2* expression compared to neovascularized *Dcn*$^{+/+}$ mice corneas. (B) *Timp1* mRNA expression was significantly reduced in neovascularized corneas *vs* naïve corneas in *Dcn*$^{-/-}$ mice and neovascularized corneas of *Dcn*$^{-/-}$ mice *vs Dcn*$^{+/+}$ mice. (C) *Vegfr2* mRNA expression was significantly reduced in neovascularized corneas *vs* naïve corneas in both the *Dcn*$^{+/+}$ and *Dcn*$^{-/-}$ mice and significantly increased in naïve corneas of *Dcn*$^{-/-}$ mice *vs Dcn*$^{+/+}$ mice. Results are expressed as mean ± SEM (One-Way ANOVA, *$p < 0.05$, **$p < 0.01$, ***$p < 0.001$, and ****$p < 0.0001$).

Table 1

Quantitative RT-PCR primer sequences.

Target gene	Forward primer 5' – 3'	Reverse primer 5' – 3'
Vegf	CAC TGG ACC CTG GCT TTA C	CTT CAT GGG ACT TCT GCT CTC
Pdgf	CTC TTG GAG ATA GAC TCC GTA GG	ACT TCT CTT CCT GCG AAT GG
Pecam	GAGCCCAATCACGTTTCAGTTT	TCCTTCCTGCTTCTTGCTAGCT
Endoglin	GCAGGTGTCAGCAAGTATGA	GAAAGAGAGGCTGTCCATGTT
Vegfr2	GGC GGT GGT GAC AGT ATC TT	TCT CCG GCA AGC TCA AT
Timp1	GATGGTGGGTGGATGAGTAATG	CCTGAGCGCTAGAGGATAAATG
Ang-2	GCTTCGGGAGCCCTCTGGGA	CAGCGAATGCGCCTCGTTGC
β-actin	CGT TGA CAT CCG TAA AGA CC	TAG GAG CCA GAG CAG TAA TC

Vegf – vascular endothelial growth factor; *Pdgf* - platelet-derived growth factor; *Pecam* - Platelet endothelial cell adhesion molecule; *Vegfr2* – VEGF receptor 2; *Timp1* - tissue inhibitors of metalloproteinase 1; *Ang-2*– Angiopoietin 2.